Contribution from the Department of Chemistry,
University of Iowa, Iowa City, Iowa 52242

Low-Spin Manganese(III) Porphyrin Imidazolate and Cyanide Complexes. Modulation of Magnetic Anisotropy by Axial Ligation

ANDREW P. HANSEN and HAROLD M. GOFF*

Received February 1, 1984

Few examples of low-spin manganese(III) complexes are known. Spin pairing in manganese(III) porphyrin derivatives is reportedly induced through binding of two strong ligand-field imidazolate ligands. Low-spin dicyanomanganese(III) porphyrin complexes are described here for the first time. An unusual autoreduction process is noted for dicyanomanganese(III) tetraarylporphyrin dimethyl sulfoxide solutions in which a high-spin manganese(II) porphyrin complex is formed. Detailed solution characterization of the two classes of low-spin manganese(III) porphyrin complexes is provided by extensive nuclear magnetic resonance measurements. The paramagnetic $S = 1$ species exhibit unusually sharp signals as expected for a low-spin d^4 ion. Pyrrole proton NMR resonances for tetraarylporphyrin derivatives are shifted to far upfield positions reminiscent of the pattern observed for low-spin iron(III) analogues. The shift patterns are consistent with expectations for a low-spin d^4 ion with unpaired spin in the π-symmetry d_{xz}, d_{yz} set and spin transfer by a porphyrin $\rightarrow$ Mn(III) mechanism. Separation of dipolar and contact shift contributions permits calculation of molecular susceptibilities for the axially symmetric complexes. Surprisingly, the axial ligands modulate magnetic anisotropy such that $\chi_{\parallel} > \chi_{\perp}$ for dicyanide ligation and $\chi_{\parallel} < \chi_{\perp}$ for diimidazolate ligation. Although the low-spin manganese(III) complexes and putative iron(IV) porphyrin hemoprotein and model compound species are isoelectronic, no parallels are seen in the magnitude of hyperfine chemical shift values or line widths. Earlier theoretical predictions that place large unpaired spin density on an oxo ligand (rather than on the porphyrin) of oxoiron(IV) complexes may explain the significantly different chemical shift values for isoelectronic complexes.

Introduction

Although the trivalent state of manganese coordination compounds is relatively rare, this oxidation state is apparent as the air-stable form of manganese porphyrin adducts. Manganese(III) porphyrins are frequently isolated from nonaqueous media with a single axial anionic ligand.[1] Simultaneous ligation by chloro and pyridine residues is possible in the solid state,[2] but electrochemical measurements and optical spectra suggest little affinity for a second nitrogenous ligand or solvent molecule.[1,3,4] In either case the d^4 manganese(III) ion exists in the high-spin $S = 2$ state. Indeed a very strong ligand field is required to induce manganese(III) spin pairing to the low-spin $S = 1$ state. Prior to 1980 the only known low-spin manganese(III) complex was that of the $[Mn(CN)_6]^{3-}$ ion.[5] More recently, the diimidazolate complex of manganese(III) tetraphenylporphyrin has been identified through solid-state magnetic measurements as a low-spin derivative.[6] Bond length correlations are also consistent with alternating low-spin manganese(III) porphyrin centers in an imidazolate-bridged polymer.[6]

Further elucidation of low-spin manganese(III) porphyrin solution properties, electronic structure, and magnetic anisotropy would clearly be desirable in view of the paucity of low-spin manganese(III) examples. Recent use of manganese porphyrins as oxidative catalysts demands that all spin and oxidation states be thoroughly characterized for reliable identification of reaction intermediates.[7] Furthermore, the low-spin d^4 metalloporphyrin is isoelectronic with the elusive iron(IV) state thought to be important as an intermediate in various hemoprotein catalysis reactions.[8] It is of interest to compare spectroscopic properties of the low-spin manganese(III) porphyrin with those of identified iron(IV) derivatives. Generation of low-spin dicyanomanganese(III) porphyrin complex ions has also been possible, despite previous statements to the contrary[1] and very low affinity for bisligation by cyanide ion in alcohol solution.[4] Solution characterization of the imidazolate and cyanide complexes has relied heavily on proton NMR spectral measurements. These studies have proven highly informative as a consequence of the favorable line widths and large signal dispersion observed for the paramagnetic low-spin d^4 ion. Detailed analysis of the chemical shift data reveals an unexpected reversal in the direction of magnetic anisotropy as the axial ligand is changed.

Experimental Section

Materials. Synthetic tetraphenylporphyrin derivatives (TPP),[9] octaethylporphyrin (OEP),[10] and etioporphyrin I (ETIO)[11] were prepared by cited literature methods. Manganese ion was incorporated by the usual dimethylformamide reflux method,[12] in which solid anhydrous manganese(II) acetate was added to a refluxing porphyrin solution exposed to the atmosphere. Following a 1-h reflux, an aqueous saturated NaCl solution was added to the cool dimethylformamide mixture. The solid product was recovered by filtration on a medium-porosity glass frit. Conversion to the chloride complex was ensured by stirring a methylene chloride solution of the manganese(III) porphyrin with an aqueous 1 M HCl solution. The organic layer was dried over $CaCl_2$ and subjected to purification on a silica gel column with methylene chloride and 4% methanol–methylene chloride eluents. After filtration of the methylene chloride eluate, solid product was recovered by rotary evaporation with slow addition of heptane. Chloromanganese(III) porphyrins were vacuum-dried at 100 °C. Integrity of the products was confirmed through visible–ultraviolet[1] and proton NMR spectral measurements.[13] Manganese analysis (by nitric acid–sulfuric acid digestion and periodate oxidation[14]) provided a quantitative basis for calculation of magnetic moment and molar absorptivity values.

Manipulations of the moisture-sensitive imidazolate salts were conducted in a Vacuum Atmospheres Corp. glovebox under a nitrogen atmosphere. Potassium salts of imidazole, 4-methylimidazole, and 2-methylimidazole (Aldrich products) were prepared by a common route. Potassium hydride (Alfa) as a 23.6% suspension in oil was

(1) Boucher, L. J. *Coord. Chem. Rev.* **1972**, *7*, 289.
(2) Kirner, J. F.; Scheidt, W. R. *Inorg. Chem.* **1975**, *14*, 2081.
(3) Kadish, K. M.; Kelly, S. *Inorg. Chem.* **1979**, *18*, 2968.
(4) Scheidt, W. R.; Lee, Y. J.; Luangdilok, W.; Haller, K. J.; Anzai, K.; Hatano, K. *Inorg. Chem.* **1983**, *22*, 1516.
(5) Cotton, F. A.; Wilkinson, G. "Advanced Inorganic Chemistry", 4th Ed.; Wiley: New York, 1980; p 744.
(6) Landrum, J. T.; Hatano, K.; Scheidt, W. R.; Reed, C. A. *J. Am. Chem. Soc.* **1980**, *102*, 6729.
(7) (a) Smegal, J. A.; Hill, C. L. *J. Am. Chem. Soc.* **1983**, *105*, 3515. (b) Groves, J. T.; Watanabe, Y.; McMurry, T. J. *J. Am. Chem. Soc.* **1983**, *105*, 4489.
(8) Hanson, L. K.; Chang, C. K.; Davis, M. S.; Fajer, J. *J. Am. Chem. Soc.* **1981**, *103*, 633 and references contained therein.
(9) Adler, A. D.: Longo, F. R.; Finarelli, J. D.; Goldmacher, J.; Assour, J.; Korsakoff, L. *J. Org. Chem.* **1967**, *32*, 476.
(10) Wang, C.-B.; Chang, C. K. *Synthesis* **1979**, 548.
(11) Fuhrhop, J.-H.; Smith, K. M. In "Porphyrins and Metalloporphyrins"; Smith, K. M., Ed.; Elsevier: Amsterdam, 1975; pp 765–769.
(12) Adler, A. D.; Longo, F. R.; Varadi, V. *Inorg. Synth.* **1976**, *16*, 213.
(13) La Mar, G. N.; Walker, F. A. *J. Am. Chem. Soc.* **1975**, *97*, 5103.
(14) Lingane, J. J. "Analytical Chemistry of Selected Metallic Elements"; Reinhold: New York, 1966; p 77.

0020-1669/84/1323-4519$01.50/0

Table I. Electronic Absorption Spectra of Manganese(III) Porphyrin Complexes[a]

complex ion	λ_{max}, nm ($10^{-3}\epsilon$, L mol^{-1} cm^{-1})
(TPP)Mn(Me_2SO)$_x^+$	375 (46.8), 397 (49.4), 415 (sh), 465 (124), 515 (13.1), 567 (17.4), 602 (15.0)
(TPP)Mn(Im)$_2^-$ [b]	380 (sh), 408 (103), 451 (125), 535 (15.2), 583 (20.4), 625 (25.5)
(TPP)Mn(CN)$_2^-$ [c]	435 (110), 545 (16.0), 668 (5.0)
(OEP)Mn(Me_2SO)$_x^+$	366 (69.3), 385 (sh), 410 (20.9), 456 (79.3), 492 (5.0), 543 (10.8), 575 (7.1), 680 (1.3), 774 (2.1)
(OEP)Mn(Im)$_2^-$	387 (55), 435 (52), 557 (12)
(OEP)Mn(CN)$_2^-$ [c]	365 (45.2), 413 (sh), 422 (53.6), 557 (8.3)

[a] Conditions: Me_2SO solvent; 25 °C; manganese porphyrin concentrations (added as the chloro adduct) typically 2×10^{-5} M. [b] KIm concentration approximately 0.05 M. [c] Saturated KCN solution; spectra were recorded immediately after dissolution to minimize effects of autoreduction.

washed with heptane. This solid was slowly added to a 25% mole excess of the imidazole contained in a tetrahydrofuran (THF) solution. An excess of imidazole was used to ensure that all the KH had reacted. Deprotonation was judged to be complete when hydrogen gas evolution had ceased. The potassium imidazolate salt precipitated from solution and was removed by filtration. The excess imidazole remained in solution, and any retained in the potassium imidazolate was removed by a THF wash.

Solvents used for glovebox work were purged with nitrogen gas and dried with activated molecular sieves. Deuterated dimethyl sulfoxide (Me_2SO-d_6) from freshly opened vials was treated in the same way.

Preparation of Samples for Spectroscopic Analysis. Manganese(III) porphyrin imidazolate and cyanide complexes were generated in situ in NMR and EPR tubes and in volumetric flasks for visible–ultraviolet measurements. This was typically accomplished by careful weighing of the chloromanganese(III) porphyrin outside the glovebox, followed by addition of solvent and ligand inside the glovebox. Samples were sealed with rubber septa during spectroscopic analysis. Titration experiments were performed with use of a gastight syringe to transfer potassium imidazolate stock solution into the septum-sealed NMR tube. Such elaborate handling of the cyanide complexes was not essential, although the presence of significant amounts of water in Me_2SO lowers the apparent binding affinity of cyanide ion.

Physical Measurements. Proton NMR spectra were recorded at 89.56 MHz on a JEOL FX-90Q Fourier transform spectrometer. Downfield shifts are given a positive sign, and tetramethylsilane (Me_4Si) serves as a standard reference substance. Deuterium and carbon resonances were recorded on the same instrument at 13.7 and 22.5 MHz, respectively. Electron paramagnetic resonance measurements were made at −180 °C on a Varian E-104A X-band instrument. Electronic spectra were taken on either a Beckman Model 25 or a Cary 219 instrument using 1–10-mm quartz cells that had been filled in the glovebox.

Results

Electronic Spectra. The electronic spectra of several high-spin manganese(III) porphyrins have been recorded.[1] When Me_2SO is employed as a solvent, weak axial ligands are displaced by solvent molecules, and all five-coordinate complexes give identical spectra.[1] Addition of imidazole up to 0.05 M produced no significant change in the (TPP)Mn(Me_2SO)$_x^+$ spectrum. However, addition of excess potassium imidazolate brings a dramatic change, as may be seen in Figure 1. Band positions are in close agreement with those previously reported for (TPP)Mn(Im)$_2^-$ in THF solution.[6] However, the molar absorptivity values in Table I are approximately fourfold higher than those of the earlier study. Values reported here are consistent with those observed for many other manganese porphyrin complexes.[1,15]

Imidazolate coordination to (OEP)Mn(Me_2SO)$_x^+$ and (ETIO)Mn(Me_2SO)$_x^+$ is also apparent on the basis of electronic spectral changes. Spectra of these structurally similar complexes are nearly identical, and results are reported only for the OEP derivative in Table I.

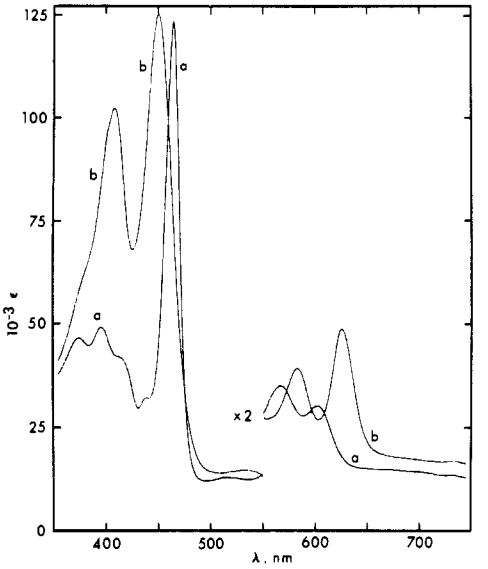

Figure 1. Electronic spectra of manganese(III) tetraphenylporphyrin complexes (Me_2SO solvent, 25 °C, 1.6×10^{-5} M manganese porphyrin): (a) (TPP)Mn(Me_2SO)$_x^+$; (b) (TPP)Mn(Im)$_2^-$ in the presence of 0.05 M KIm.

Addition of excess solid KCN to Me_2SO solutions of manganese(III) porphyrins likewise brings striking spectral changes as may be noted from Table I. A Soret band at 435 nm for the presumed dicyano (TPP)Mn^{III} adduct is clearly different from those reported at 405 and 495 nm for the monocyano (TPP)Mn^{III} complex.[16] It will be shown through interpretation of other physical measurements that electronic spectral changes are associated with imidazolate and cyanide ligation, and subsequent conversion to the low-spin manganese(III) state.

Magnetic Measurements. Solution magnetic measurements were made by the NMR (Evans) method[17] with use of a capillary insert and Me_4Si as a reference substance. Diamagnetic corrections have been based on the susceptibility reported for the free TPP ligand[18] and appropriate Pascal constants. Values for the low-spin complexes examined here at 25 °C are as follows: K[(TPP)Mn(Im)$_2$], 3.7 ± 0.2 μ_B; K[(TPP)Mn(CN)$_2$], 3.0 ± 0.2 μ_B; K[(OEP)Mn(Im)$_2$], 3.0 ± 0.2 μ_B. These solution results are to be compared with solid-state measurements for Bu_4N[(TPP)Mn(Im)$_2$] of 3.2 μ_B[6] and for $K_3Mn(CN)_6$ of 3.5 μ_B.[19] By comparison, the high-spin manganese(III) porphyrin has a magnetic moment of 4.9 μ_B.[1] Observed magnetic moments for the low-spin complexes are elevated with respect to the spin-only value of 2.83 μ_B for an $S = 1$ ion. In the limit of octahedral symmetry the T ground state for an $S = 1$ d^4 ion is expected to exhibit significant spin–orbit coupling with consequent increase in the magnetic moment.

Proton NMR Spectroscopy of Imidazolate Complexes. The structure and numbering scheme for the imidazolate ion is shown:

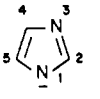

(15) Boucher, L. J. *J. Am. Chem. Soc.* **1970**, *92*, 2725.

(16) Wayland, B. B.; Olson, L. W.; Siddiqui, Z. U. *J. Am. Chem. Soc.* **1976**, *98*, 94.
(17) Evans, D. F. *J. Chem. Soc.* **1959**, 2003.
(18) Eaton, S. S.; Eaton, G. R. *Inorg. Chem.* **1980**, *19*, 1095.
(19) Figgis, B. N. "Introduction to Ligand Fields"; Interscience: New York, 1966; p 287.

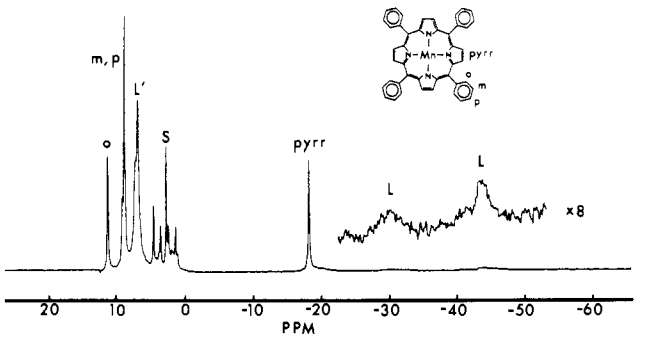

Figure 2. Proton NMR spectrum of $(TPP)Mn(Im)_2^-$ (Me_2SO-d_6 solvent, 26 °C, 0.01 M manganese porphyrin, 0.1 M KIm). Upfield signals labeled "L" are for coordinated imidazolate residues, the "S" signal is for the solvent, and the "L'" signals are for free imidazolate ion. Additional minor signals in the diamagnetic region are for THF of crystallization in KIm and for heptane retained in (TPP)MnCl.

Potassium imidazolate salts were found to have adequate solubility in Me_2SO for the necessary NMR experiments. Use of the potassium vs. the tetrabutylammonium salt was desirable in that fewer extraneous proton signals were introduced upon ligand addition. Addition of approximately 1 equiv of KIm to manganese(III) porphyrins resulted in formation of solid material that is presumed to be the polymeric imidazolate-bridged species.[6] However, addition of approximately 10 equiv of KIm produced a homogeneous solution species with the proton NMR spectrum shown in Figure 2. The phenyl proton signals of TPP were assigned by examination of *m*- and *p*-methyl analogues. The upfield pyrrole proton signal was relatively invariant for the several derivatives and showed no hint of splitting or broadening for the *m*-methyl derivative. The downfield peak assigned to the *o*-phenyl proton consisted of two closely spaced components for the *m*-methyl $(TPP)Mn^{III}$ complex.

Two small broad signals were observed far upfield of Me_4Si. Comparison of areas revealed that each signal had one-fourth the intensity of ortho phenyl and β-pyrrole proton signals. Assignment of the two signals to coordinated imidazolate appears reasonable. A 2:1 ligand:manganese stoichiometry is thus established. Furthermore, appearance of both free and coordinated imidazolate signals indicates that ligand exchange between Im^- and $(TPP)Mn(Im)_2^-$ is not rapid on the NMR time scale. The third coordinated imidazolate signal has not been assigned but presumably is located in the 0–10-pm region.

Use of 4-methylimidazolate permits generation of only partially ligated solution mixtures, as proximity of the methyl group diminishes the tendency for formation of imidazolate bridges. Proton NMR spectra at various concentrations of 4-methylimidazolate are shown in Figure 3. Dramatic line width changes are observed upon conversion of the high-spin manganese(III) complex to the low-spin state; the pyrrole proton signal for the Me_2SO complex (Figure 3a) is 1000 Hz wide, whereas the corresponding bis(4-methylimidazolate) complex signal (Figure 3d) is 25 Hz wide. At intermediate 4-methylimidazolate concentrations all signals are broad and migrate toward the low-spin chemical shift values as the total ligand concentration increases. This implies rapid exchange between $(TPP)Mn(4\text{-}CH_3Im)_2^-$ and $(TPP)Mn(Me_2SO)_x^+$ or more likely existence of a mono(4-methylimidazolate) complex that is involved in rapid ligand exchange. Observation of far upfield coordinated 4-methylimidazolate signals as well as the downfield 4-methyl signal confirms assignment of the upfield 2,5-proton resonances. The fact that bound 4-methylimidazolate signals are not split confirms that the ligand is bound through only one type of nitrogen residue—most likely the 1-nitrogen atom. Binding of 2-methylimidazolate to give a low-spin complex was not detected under the concentration

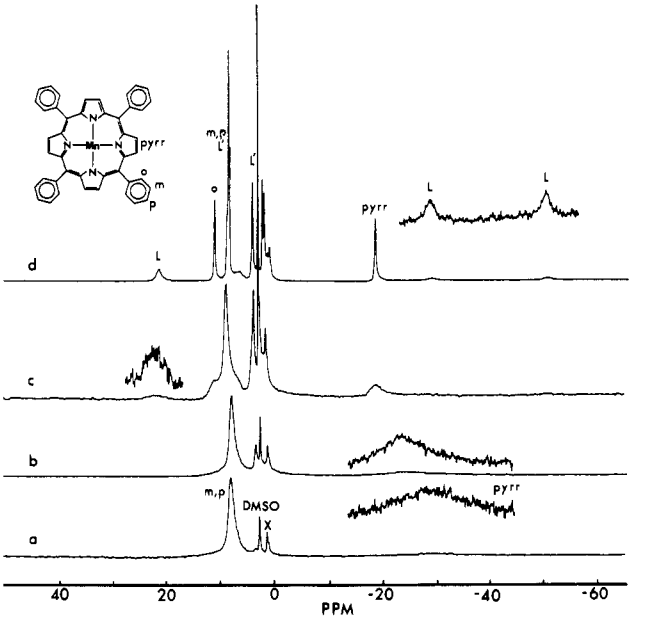

Figure 3. Proton NMR spectra for the titration of $(TPP)Mn(Me_2SO)_x^+$ with $4\text{-}CH_3Im^-$ (Me_2SO-d_6 solvent, 26 °C, 0.01 M manganese porphyrin): (a) $(TPP)Mn(Me_2SO)_x^+$ with no $4\text{-}CH_3Im^-$ present; (b) 2.0 equiv of K(4-CH_3Im) added; (c) 5.0 equiv of K(4-CH_3Im) added; (d) 10.0 equiv of K(4-CH_3Im) added. Signals labeled "L" are for coordinated $4\text{-}CH_3Im^-$ residues, the "L'" signals are for free $4\text{-}CH_3Im^-$, and the "X" signals are for heptane retained in (TPP)MnCl.

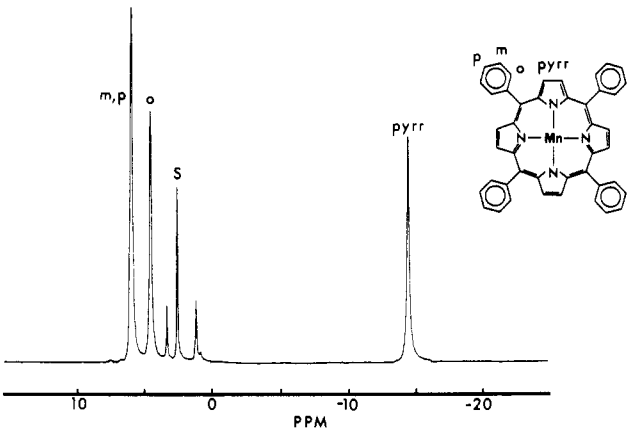

Figure 4. Proton NMR spectrum of $(TPP)Mn(CN)_2^-$ (Me_2SO-d_6 solvent, 26 °C, 0.01 M manganese porphyrin, solution saturated with KCN). The "S" signal is for Me_2SO solvent. Other minor signals in the diamagnetic region are from water (at 3.3 ppm) and heptane retained in solid (TPP)MnCl.

conditions of Figure 3, indicating the severe steric constraints of a methyl group on the carbon atom adjacent to the coordinated nitrogen atom.

Imidazolate complexes of $(OEP)Mn^{III}$ and $ETIOMn^{III}$ are generated under the same conditions as those for $(TPP)Mn^{III}$. Peak assignments are made quite simply on the basis of peak areas and by comparison of chemical shift values for the two structurally related porphyrins. Peak positions are listed in Table II. Low solubilities of these porphyrin complexes precluded detection of coordinated imidazolate signals.

Proton NMR Spectroscopy of Cyanide Complexes. Proton NMR spectra of the cyanide complexes of manganese(III) porphyrins are similar to those of the respective imidazolate complexes. The spectrum of $(TPP)Mn(CN)_2^-$ is shown in Figure 4. Phenyl proton assignments were made by examination of *m*- and *p*-methyl TPP derivatives, and results are summarized in Table II. The upfield pyrrole proton signal

Table II. Proton NMR Chemical Shift Values for Manganese(III) Porphyrin Complexes[a]

Mn(III) tetraarylporphyrins	pyrr H	*o*-H	*m*-H	*p*-H	Ph CH_3	coord Im^- H	coord Im^- CH_3
$(TPP)Mn(Me_2SO)_x^+$	−31	*b*	7.8	7.8			
$(TPP)Mn(Im)_2^-$	−18.1	11.1	8.6	8.6		−31, −44	
$(TPP(p\text{-}CH_3))Mn(Im)_2^-$	−18.3	11.0	8.57		3.08	−31, −44	
$(TPP(m\text{-}CH_3))Mn(Im)_2^-$	−18.0	10.8	8.4	8.4	3.27	*c*	
$(TPP(p\text{-}OCH_3))Mn(Im)_2^-$	−17.9	10.9	8.1		4.54	*c*	
$(TPP)Mn(4\text{-}CH_3Im)_2^-$	−18.1	11.1	8.6	8.6		−28, −49	21.6
$(TPP)Mn(CN)_2^-$	−14.7	4.29	5.73	5.73			
$(TPP(p\text{-}CH_3))Mn(CN)_2^-$	−14.1	4.26	5.53		1.25		
$(TPP(m\text{-}CH_3))Mn(CN)_2^-$	−14.3	4.22	5.66	5.66	1.25		

Mn(III) octaalkylporphyrins	methine H	ring CH_3	ring CH_2	Et CH_3
$(OEP)Mn(Me_2SO)_x^+$	76		13.6	2.0
$(OEP)Mn(Im)_2^-$ [c]	48.6	(31.2)	14.2	3.24
$(OEP)Mn(CN)_2^-$	33.9	(15.6)	4.4	−0.42
$(ETIO)Mn(CN)_2^-$	36.0	16.0	4.8	−0.45

[a] Conditions: Me_2SO-d_6 solvent; 26 °C; Mn(III) tetraarylporphyrins typically 0.01 M; Mn(III) tetraalkylporphyrins typically 0.005 M; excess imidazolate salts 0.05–0.1 M; solutions for cyanide complexes saturated with KCN. [b] The *o*-phenyl signal is broadened severely and presumably overlaps with other phenyl signals. [c] Inadequate signal/noise precluded reliable location of coordinated imidazolate signals.

at −14.2 ppm is to be compared with a value of −18.1 ppm for $(TPP)Mn(Im)_2^-$. Significant differences are observed in the phenyl proton chemical shift values for the two complexes. An upfield bias is apparent for the phenyl proton signals of $(TPP)Mn(CN)_2^-$ with the ortho proton resonance at 4.4 ppm. The corresponding signal for $(TPP)Mn(Im)_2^-$ is at 11.1 ppm. These differences will subsequently be analyzed in terms of the magnetic anisotropy of the two types of complexes (vide infra).

Differences also exist for proton NMR spectra of cyanide vs. imidazolate complexes of $(OEP)Mn^{III}$ and $(ETIO)Mn^{III}$. A greater downfield bias is apparent for signals of the imidazolate adducts. For example, the CH_3 signals for ethyl groups in the cyanide complexes are slightly upfield from Me_4Si, whereas the corresponding signal is at 3.2 ppm in $(OEP)Mn(Im)_2^-$. Spectra of the cyanide species are shown in Figure 5, and results are summarized in Table II.

The stoichiometry for cyanide binding has been inferred only indirectly. Stoichiometry determination through stepwise addition of potassium cyanide with monitoring by optical and NMR spectroscopy was complicated by simultaneous autoreduction of the $(TPP)Mn(CN)_2^-$ complex (vide infra) and probable appearance of a monocyano complex. Ligation by two cyanide ions in the low-spin complexes is supported by two observations. The previously reported[4,16] monocyano $(TPP)Mn^{III}$ complex is high spin and exhibits an optical spectrum much different from that observed when excess cyanide ion is present. It thus appears that insufficient ligand field is provided by one axial cyanide ion (and possibly a solvent molecule) to induce spin pairing. Proton NMR results are also consistent with symmetrical ligation by two cyanide ions. Ligation by one axial anionic ligand in general brings splitting of phenyl proton signals in paramagnetic TPP derivatives and splitting of diastereotopic ring methylene signals in paramagnetic metallooctaalkylporphyrins.[20,21] No indication of such splittings was apparent for the presumed dicyanomanganese(III) porphyrins.

An anomalous peak is noted at 15.6 ppm in the proton NMR spectrum of $(OEP)Mn(CN)_2^-$. This extra signal, which is about 2% the intensity of the ring-CH_2 resonance, is also noted at 31.2 ppm for the $(OEP)Mn(Im)_2^-$ complex. Presence of the minor signals is invariant with addition of variable amounts of ligands and temperature changes, thus indicating that the signals are not due to trace equilibrium components.

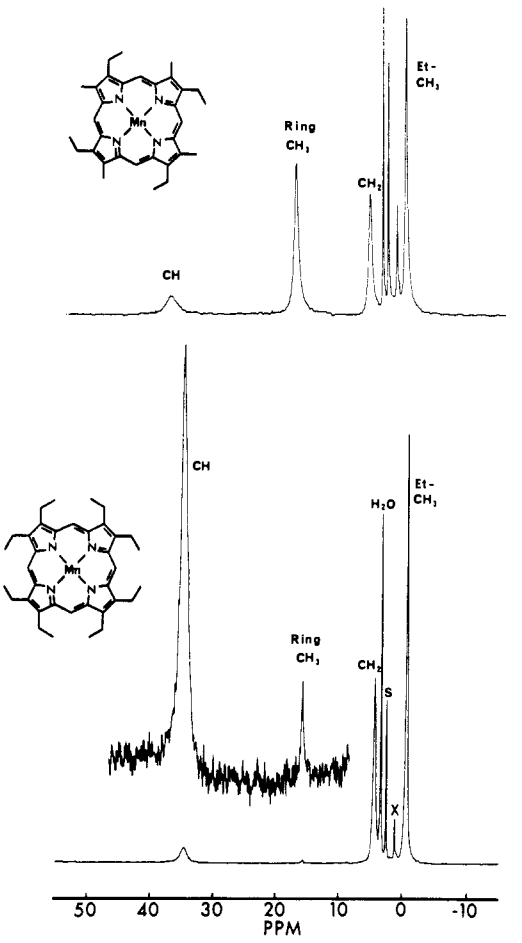

Figure 5. Proton NMR spectra of dicyano complexes of manganese(III) octaalkylporphyrins (Me_2SO-d_6 solvent, 26 °C, 0.005 M manganese porphyrin, solutions saturated with KCN). The "S" signal is for Me_2SO solvent; the "X" signal represents heptane retained in the solid chloromanganese(III) compounds.

The minor signal at 15.6 ppm matches in position that for the ring methyl peak of $(ETIO)Mn(CN)_2^-$. It is thus likely that in the synthesis of OEP by the method of Wang and Chang[10] a small amount (perhaps 1–2%) of the 4,5-diethyl-3-methylpyrrole is formed rather than the desired 3,4-diethyl-5-methylpyrrole OEP precursor.[22] This complication has not been noted previously and became apparent in the present

(20) La Mar, G. N.; Walker, F. A. In "The Porphyrins"; Dolphin, D., Ed.; Academic Press: New York, 1979; Vol. IV, pp 61–157.
(21) Goff, H. M. In "Iron Porphyrins"; Lever, A. B. P., Gray, H. B., Eds.; Addison-Wesley: Reading, MA, 1982; Part I, pp 237–281.
(22) Purification of the pyrrole by distillation is now recommended: Chang, C. K., private communication.

study as a consequence of the favorable dispersion of ring methyl and methylene signals from the diamagnetic region (where appearance of a minor signal might be attributed to a trace organic contaminant).

Autoreduction of Cyanide Complexes. Over a period of hours solutions of the red-brown cyanide complexes of (TPP)Mn^{III} changed to a bright green color. This process has not been studied in detail, but the green product was clearly identified as a manganese(II) species on the basis of the following magnetic, EPR, NMR, and oxygenation experiments. The solution of (TPP)$Mn(CN)_2^-$ prepared for a magnetic moment determination was examined shortly after mixing, and a magnetic moment of 3.0 μ_B was measured. Upon standing for 1 day, the solution turned bright green, and the magnetic moment determination revealed a value of 5.8 $\pm$ 0.2 μ_B. This is consistent with a spin-only value of 5.92 μ_B expected for a high-spin d^5 manganese ion. The EPR scan of a (TPP)$Mn(CN)_2^-$ solution in frozen Me_2SO at −180 °C initially showed no signals. However, as the sample was thawed and heated at 80 °C for intervals of a few minutes, subsequent EPR spectra recorded at −180 °C contained broad $g = 6$ and $g = 2$ features attributable to high-spin manganese(II). A deuterium NMR experiment further confirmed the identity of the bright green reduced product. Cyanide complexes of (TPP-pyrrole-d_8)Mn^{III} and (TPP-phenyl-d_{20})-Mn^{III} were converted to the green product, and deuterium NMR spectra revealed phenyl signals centered at 6.7 ppm and a pyrrole signal at 36 ppm diagnostic of the manganese(II) species.[23] The manganese(II) product in Me_2SO exhibited optical spectral bands at 438 (Soret), 571, and 610 nm. These values may be compared to those of (TPP)Mn^{II} dissolved in THF at 434, 524, 566, and 603 nm.[24] After 3 days of oxygen bubbling of this solution, the spectrum of (TPP)$Mn(Me_2SO)_x^+$ (with a major Soret band at 465 nm) was recovered. Thus, the added KCN was eventually consumed in a catalytic cycle that returns the manganese porphyrin to the +3 state. The autoreduction process for (TPP)$Mn(CN)_2^-$ in Me_2SO parallels that previously observed for the iron(III) analogue, (TPP)-$Fe(CN)_2^-$.[25]

Carbon-13 NMR Measurements. Efforts were made to obtain carbon-13 NMR spectra of the low-spin manganese(III) porphyrin complexes. However, limited solubility and reduction of the cyanide complex during data acquisition complicated a full carbon-13 study. Observation and unambiguous assignment of the (TPP)$Mn(4\text{-}CH_3Im)_2^-$ porphyrin methine carbon resonance at −11.7 ppm (26 °C, Me_4Si reference, Me_2SO solvent) were possible through use of a 60 atom % methine porphyrin carbon-13 labeled derivative. The large upfield chemical shift apparent for this carbon atom is highly relevant to the discussion of unpaired spin delocalization in low-spin manganese(III) porphyrin complexes (vide infra).

Discussion

Calculation of Magnetic Anisotropy. Chemical shift values for a paramagnetic complex differ from those of the corresponding diamagnetic complex by a quantity known as the isotropic (or hyperfine) shift value. Diamagnetic bis(imidazole)cobalt(III) porphyrin complexes[26] were utilized as reference compounds in this study. The isotropic shift is composed of contact and dipolar shift contributions:

$$\frac{\Delta H_{iso}}{H} = \frac{\Delta H_{con}}{H} + \frac{\Delta H_{dip}}{H} \qquad (1)$$

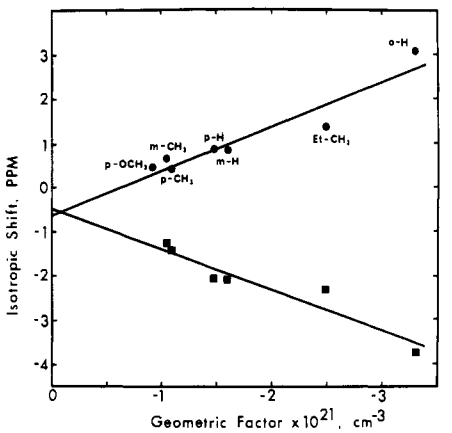

Figure 6. Graphical results demonstrating the correspondence between selected isotropic shift values and geometric factors. Low-spin manganese(III) porphyrin signals are labeled for Me_2SO-d_6 solutions at 26 °C where analogous cobalt(III) diimidazole complexes have been used as diamagnetic reference compounds. Circles (●) represent diimidazole complexes, and squares (■) represent dicyano complexes.

Unpaired spin delocalization (and polarization) through chemical bonds defines the magnitude of the contact term. In the limit of axial symmetry and insignificant contributions from ligand-centered spin density, the through-space dipolar term from metal-centered unpaired spin is defined by[27]

$$\frac{\Delta H_{dip}}{H} = \frac{1}{3N}(\chi_{\parallel} - \chi_{\perp})\frac{3\cos^2\theta - 1}{r^3} \qquad (2)$$

where N is Avogadro's number and χ values refer to molecular susceptibilities. The $(3\cos^2\theta - 1)/r^3$ "geometric factor" defines the position of the observed nucleus with respect to the molecular axis and metal center.

Separation of contact and dipolar terms is an essential first step for gaining detailed magnetic and spin delocalization information from NMR spectra. In favorable cases this is accomplished by virtue of the expectation that phenyl protons of TPP complexes are isolated from contact spin density and accordingly experience only dipolar shifts. As such, a plot of isotropic shifts vs. geometric factors (calculated from X-ray molecular structures) for phenyl nuclei should yield a linear plot with a zero intercept and a slope of $(1/3N)(\chi_{\parallel} - \chi_{\perp})$. This methodology has been applied for both proton[28,29] and carbon[26,30] spectroscopy of low-spin iron(III) and low-spin cobalt(II) porphyrin complexes, and for proton spectra of intermediate-spin[31] and high-spin[32,33] iron(II) porphyrin complexes. Graphical results for the low-spin manganese(III) porphyrin derivatives are presented in Figure 6. Data are combined for TPP, for phenyl-substituted TPP derivatives, and for the methyl proton signal of OEP complexes. It is immediately obvious that signs of the quantities $\chi_{\parallel} - \chi_{\perp}$ are opposite for imidazolate and cyanide complexes. The net susceptibility, $\bar{\chi}$, is obtained from

$$\mu_{eff} = 2.83(\bar{\chi}T)^{1/2} \qquad (3)$$

Individual $\chi_{\parallel}$ and $\chi_{\perp}$ values are estimated from slopes in Figure 6 and the relationship for axial symmetry

$$\bar{\chi} = \tfrac{1}{3}(\chi_{\parallel} + 2\chi_{\perp}) \qquad (4)$$

(23) Shirazi, A.; Goff, H. M. *J. Am. Chem. Soc.* **1982**, *104*, 6318.
(24) Reed, C. A.; Kouba, J. K.; Grimes, C. J.; Cheung, S. K. *Inorg. Chem.* **1978**, *17*, 2666.
(25) (a) Del Gaudio, J.; La Mar, G. N. *J. Am. Chem. Soc.* **1976**, *98*, 3014. (b) La Mar, G. N.; Del Gaudio, J. *Adv. Chem. Ser.* **1977**, *No. 162*, 207.
(26) Goff, H. M. *J. Am. Chem. Soc.* **1981**, *103*, 3714.
(27) Horrocks, W. D. In "NMR of Paramagnetic Molecules"; La Mar, G. N., Horrocks, W. D., Holm, R. H., Eds.; Academic Press: New York, 1973; pp 127–177.
(28) La Mar, G. N.; Walker, F. A. *J. Am. Chem. Soc.* **1973**, *95*, 1782.
(29) La Mar, G. N.; Walker, F. A. *J. Am. Chem. Soc.* **1973**, *95*, 1790.
(30) Shirazi, A.; Goff, H. M. *Inorg. Chem.* **1982**, *21*, 3420.
(31) Goff, H.; La Mar, G. N.; Reed, C. A. *J. Am. Chem. Soc.* **1977**, *99*, 3641.
(32) Goff, H.; La Mar, G. N. *J. Am. Chem. Soc.* **1977**, *99*, 6599.
(33) Parmely, R. C.; Goff, H. M. *J. Inorg. Biochem.* **1980**, *12*, 269.

Table III. Separation of Chemical Shift Terms[a]

	$\Delta H_{obsd}/H$	$\Delta H_{diamag}/H$	$\Delta H_{iso}/H$	$\Delta H_{dip}/H$	$\Delta H_{con}/H$	A^H, MHz	ρ_C^π
			PorMn(Im)$_2^-$				
pyrr H	−18.1	9.07	−27.2	6.41	−33.6	−0.48	0.015
methine H	48.6	10.25	38.3	10.38	27.9	0.40	−0.013
pyrr CH_3	31.2	3.70	27.5	3.62	23.9		
Im$^-$ H	−31	−0.2	−31	−22	−9		
Im$^-$ H	−44	−0.2	−44	−22	−22		
			PorMn(CN)$_2^-$				
pyrr H	−14.7	9.07	−23.8	−6.97	−16.8	−0.24	0.0076
methine H	33.9	10.25	23.6	−10.66	34.3	0.49	−0.015
pyrr CH_3	16.0	3.70	12.3	−4.4	16.7		

[a] Conditions: Me_2SO-d_6 solvent; 26 °C; diamagnetic references are for analogous bis(imidazole)cobalt(III) porphyrin complexes.

For (TPP)Mn(Im)$_2^-$ $\chi_\parallel = 4500 \times 10^{-6}$ cgsu and $\chi_\perp = 6300 \times 10^{-6}$ cgsu, whereas for (TPP)Mn(CN)$_2^-$ $\chi_\parallel = 4900 \times 10^{-6}$ cgsu and $\chi_\perp = 3200 \times 10^{-6}$ cgsu.

Regardless of the exact value of calculated molecular susceptibilities, it is apparent that imidazolate and cyanide ligand interactions are sufficiently different to induce reversal in the magnitude of $\chi_\parallel$ and $\chi_\perp$ values. This is a curious although not unique phenomenon. Less dramatic modulation of magnetic anisotropy by axial ligands has been previously recognized for one other class of metalloporphyrin complexes. Five-coordinate high-spin iron(II) porphyrin complexes exhibit an ordering of $\chi_\parallel > \chi_\perp$ for axial imidazole ligands and $\chi_\perp > \chi_\parallel$ for aliphatic mercaptide ligands.[33] It is apparent that NMR methods are more widely applicable to eludication of such fundamental magnetic properties, as compared with magnetic susceptibility and EPR methods that respectively require large crystals or an odd-spin electronic configuration.

Unpaired Spin Delocalization. The anticipated d-orbital configuration for a low-spin manganese(III) porphyrin complex with D_{4h} symmetry is $(d_{xy})^2$, $(d_{xz}, d_{yz})^2$, $(d_{z^2})^0$, $(d_{x^2-y^2})^0$. Unpaired spin in only the π-interacting e_g $(d_{xz}, d_{yz})^2$ orbital set leads to the expectation of large π-type unpaired spin delocalized into the macrocycle. Available porphyrin orbitals of e symmetry include the filled $3e(\pi)$ MO and the vacant $4e(\pi)$ MO.[34] The $3e(\pi)$ MO has large amplitudes at pyrrole carbon positions and zero (or possibly negative amplitude if electron correlation effects are considered) at the methine position. The $4e(\pi)$ wave function has a very large positive amplitude at the methine carbon atom and diminished values at pyrrole carbon positions.

The magnitude of unpaired spin density at proton-bearing carbon atoms may be estimated if it is assumed that spin delocalization is entirely through the π system. The proton hyperfine coupling constant, A^H, is a function of the unpaired spin density, ρ_C^π, centered on the π MO of the carbon atom to which it is attached:[26,35]

$$A^H = \frac{Q_{CH}{}^H \rho_C{}^\pi}{2S} \tag{5}$$

The empirical value of $Q_{CH}{}^H$ is approximately −63 MHz.[35] Provided the Curie law is obeyed, the correspondence between contact shift and A^H is given by

$$\frac{\Delta H_{con}}{H} = A^H \left|\frac{\gamma_e}{\gamma_H}\right| \frac{S(S+1)}{3kT} \tag{6}$$

Contact shift values for pyrrole and methine hydrogens are obtained by subtraction of dipolar terms (estimated through extrapolation of curves in Figure 6) from the isotropic shifts. Values are summarized in Table III along with the calculated carbon atom spin densities for both imidazolate and cyanide complexes. Significant unpaired spin density at the β-pyrrole carbon atom and negative spin density at the methine carbon atom suggest involvement of the filled $3e(\pi)$ porphyrin MO, such that spin transfer is by a porphyrin → Mn(III) mechanism. A 0.015 spin density at the β-pyrrole carbon atom for (TPP)Mn(Im)$_2^-$ is to be compared with a value of 0.012 for the low-spin d^5 bis(imidazolato)iron(III) tetraphenylporphyrin complex.[26] Proton NMR measurements for natural-derivative iron(III) porphyrins reveal that unpaired spin density at β-pyrrole positions is reduced upon deprotonation of coordinated imidazole ligands.[36] If an average chemical shift of −11.8 ppm for the 2,4-proton signals of the iron(III) deuteroporphyrin diimidazolate complex is considered, a spin density value of 0.010 is calculated for the β-pyrrole carbon atom. Thus, the $S = 1$ low-spin manganese(III) derivative yields somewhat more unpaired porphyrin spin density as compared with that for the $S = {}^1/_2$ iron(III) analogue.

A surprisingly large amount of negative spin density is found at the methine carbon atom of (OEP)Mn(Im)$_2^-$ (−0.013), as compared with the value of −0.0015 for the bis(imidazolato)iron(III) complex[26] (methine proton signals were not reported for the iron(III) porphyrin imidazolate complexes[36]). The significant negative spin density at the methine carbon is fully consistent with a large upfield shift to −11.7 ppm observed for the methine carbon signal in (TPP)Mn(Im)$_2^-$. Upgraded calculations that include electron correlation effects are clearly needed to provide a more realistic molecular orbital description that can address appreciable negative spin density in paramagnetic metalloporphyrin complexes.

Comparison with Iron(IV) Porphyrin NMR Spectra. It is generally accepted that low-spin iron(IV) intermediates are present during the redox cycle of peroxidases and other hemoproteins.[8] These d^4 ions are isoelectronic with low-spin manganese(III) complexes described here, and it is of interst to compare NMR spectral patterns. Proton NMR spectra of the iron(IV) compound II or horseradish peroxidase surprisingly show few signals outside the usual diamagnetic region.[37] Broad resonances near 15 ppm have recently been assigned to methine protons.[38] Perhaps the greatest similarity between the low-spin manganese(III) spectra and compound II spectra are the relatively large downfield methine proton chemical shifts.

The best defined iron(IV) model compound is formed at low temperature by 1-methylimidazole cleavage of a peroxoiron(III) tetraarylporphyrin dimer.[38-41] Proton NMR signals for

(34) Longuet-Higgins, H. C.; Rector, C. W.; Platt, J. R. *J. Chem. Phys.* **1950**, *18*, 1174.
(35) Karplus, M.; Fraenkel, G. K. *J. Chem. Phys.* **1961**, *35*, 1312.
(36) Chacko, V. P.; La Mar, G. N. *J. Am. Chem. Soc.* **1982**, *104*, 7002.
(37) Morishima, I.; Ogawa, S.: (a) *J. Am. Chem. Soc.* **1978**, *100*, 7125; (b) *Biochem. Biophys. Res. Commun.* **1978**, *83*, 946; (c) *Biochemistry* **1978**, *17*, 4384.
(38) La Mar, G. N.; de Ropp, J. S.; Latos-Grazynski, L.; Balch, A. L.; Johnson, R. B.; Smith, K. M.; Parish, D. W.; Cheng, R.-J. *J. Am. Chem. Soc.* **1983**, *105*, 782.

this species at low temperature are barely shifted from the aromatic region; the pyrrole proton signal is at 5 ppm and phenyl signals are shifted less than 2 ppm downfield. In contrast, the pyrrole proton contact shift for the presumably isoelectronic $(TPP)Mn(Im)_2^-$ is −33.6 ppm and that for $(TPP)Mn(CN)_2^-$ is −16.8 ppm at ambient temperature. Absence of significant isotropic shifts for the iron(IV) model compound and for HRP compound II has been explained by INDO–SCF[42] and extended Hückel[8] calculations that reveal efficient mixing of d_{xz}, d_{yz} orbitals with p_x, p_y orbitals of a coordinated oxo ligand. Unpaired spin density is thus localized on the oxo group at the expense of spin density transfer to the macrocycle. Data for the low-spin manganese(III) complexes can be construed as being supportive of this hypothesis. Diminished spin density at the β-pyrrole carbon atom of $(TPP)Mn(CN)_2^-$ as compared with that for $(TPP)Mn(Im)_2^-$ suggests much more efficient delocalization of spin into the cyano residue. This appears to be the case on the basis of much greater carbon-13[43] and nitrogen-15[44] chemical shifts observed for the cyano ligand vs. those for the imidazole ligand.[26] Axial ligands should thus compete with the porphyrin for unpaired spin density in the following order: oxo > cyanide > imidazolate. The oxidized cytochrome *c* peroxidase enzyme exhibits proton isotropic shifts of greater magnitude than those for horseradish peroxidase compound II.[45] Among the possible explanations for this difference is the expectation that an iron(IV) ligand such as OH^- would leave greater unpaired spin on the porphyrin, as is the case for low-spin manganese(III) complexes described here.

Acknowledgment. Support from National Science Foundation Grant CHE 82-09308 is gratefully acknowledged.

(39) Chin, D.-H.; Balch, A. L.; La Mar, G. N. *J. Am. Chem. Soc.* **1980**, *102*, 1446.
(40) Simonneaux, G.; Scholz, W. F.; Reed, C. A.; Lang, G. *Biochim. Biophys. Acta* **1982**, *716*, 1.
(41) Penner-Hahn, J. E.; McMurry, T. J.; Renner, M.; Latos-Grazynski, L.; Eble, K. S.; Davis, I. M.; Balch, A. L.; Groves, J. T.; Dawson, J. H.; Hodgson, K. O. *J. Biol. Chem.* **1983**, *258*, 12761.
(42) Loew, G. H.; Herman, Z. S. *J. Am. Chem. Soc.* **1980**, *102*, 6175.
(43) Goff, H. *J. Am. Chem. Soc.* **1977**, *99*, 7723.
(44) (a) Morishima, I.; Inubushi, T. *J. Chem. Soc., Chem. Commun.* **1977**, 616. (b) Morishima, I.; Inubushi, T.; Neya, S.; Ogawa, S.; Yonezawa, T. *Biochem. Biophys. Res. Commun.* **1977**, *78*, 739. (c) Morishima, I.; Inubushi, T. *J. Am. Chem. Soc.* **1978**, *100*, 3568.
(45) Satterlee, J. D.; Erman, J. E. *J. Biol. Chem.* **1981**, *256*, 1091.

Contribution from the Department of Chemistry, University of the Western Cape, Private Bag X17, Bellville 7530, Republic of South Africa, and Department of Physical Chemistry, University of Cape Town, Rondebosch 7700, Republic of South Africa

Reaction Pathways from Structural Data: Dynamic Stereochemistry of Nickel Compounds

THOMAS P. E. AUF DER HEYDE*† and LUIGI R. NASSIMBENI‡

Received April 26, 1984

The principle of structure correlation is applied to the crystal structures of 78 different five-coordinate nickel complexes. The data derived map the reaction coordinate for an association reaction at planar, four-coordinate nickel centers, leading to a square-pyramidal intermediate. It is shown that this intermediate may undergo pseudorotation to a trigonal-bipyramidal conformation, in which axial dissociation may occur.

Introduction

Square-planar coordination is well established amongst the metals of the nickel triad, but it is the chemistry of platinum and palladium compounds, rather than that of nickel, that has been more extensively investigated. Complexes of square-planar geometry may undergo isomerization and substitution reactions, which have been proposed to proceed via an essentially similar associative mechanism:[1,2]

$$XML_3 + Y \rightleftarrows [XML_3Y] \rightleftarrows X + ML_3Y$$

where X, L represent any ligand donor atoms and Y is X, L, or solvent. The rate of this reaction may be determined by either the associative or the dissociative step, or a combination of both. The nature of the five-coordinate intermediate has been the subject of much discussion, with earlier suggestions[1] being that it has a trigonal-bipyramidal conformation (TBP), as opposed to a square-pyramidal (SQP) one, put forward more recently.[2] It has been suggested, and in many cases shown,[1,2] that the five-coordinate intermediate $[XML_3Y]$ may undergo the fluxional behavior typical of many pentacoordinate compounds, best described by the Berry mechanism[3] shown in Figure 1. This mechanism interconverts two trigonal bipyramids (TBP) via a square pyramid (SQP) by simultaneous in-plane bends of the axial ligands (atoms 1 and 5 in Figure 1) and the equatorial ligands (atoms 2 and 4).

In this paper we apply the method of structure correlation analysis[4,5] to five-coordinate nickel complexes. We view the results as mapping the reaction coordinates for an association reaction at planar four-coordinate nickel centers resulting in a SQP intermediate, with subsequent pseudorotation and dissociation of the five-coordinate species. In terms of the structure correlation approach one examines the *gradual distortion* that a specific fragment (in this case $[NiL_5]$) undergoes in a variety of crystal environments. This distortion is then assumed to mirror the distortion which that fragment would exhibit along a particular reaction pathway. Most recently this method has been applied to an examination of the "ring-whizzing" phenomenon in complexes of the type $[(Ph_3C_3)M(PPh_3)_2]^+$, where M = Ni, Pd, Pt,[6] the stereoisomerization path for triphenylphosphine,[7] conformational dy-

†University of the Western Cape.
‡University of Cape Town.

(1) Basolo, F.; Pearson, R. G. "Mechanisms of Inorganic Reactions", 2nd ed.; Wiley: New York, 1967.
(2) Anderson, G. K.; Cross, R. J. *Chem. Soc. Rev.* **1980**, *9*, 185.
(3) Berry, R. S. *J. Chem. Phys.* **1960**, *32*, 933.
(4) Bürgi, H. B. *Angew. Chem.* **1975**, *87*, 461; *Angew. Chem., Int. Ed. Engl.* **1975**, *14*, 460. Dunitz, J. D. "X-ray Analysis and the Structure of Organic Molecules"; Cornell University Press: Ithaca, NY, 1979.
(5) Bürgi, H. B.; Dunitz, J. D. *Acc. Chem. Res.* **1983**, *16*, 153.
(6) Mealli, C.; Midollini, S.; Moneti, S.; Sacconi, L.; Silvestre, J.; Albright, T. A. *J. Am. Chem. Soc.* **1982**, *104*, 95.
(7) Bye, E.; Schweizer, W. B.; Dunitz, J. D. *J. Am. Chem. Soc.* **1982**, *104*, 5893.

0020-1669/84/1323-4525$01.50/0